Received: 3 May 2018 | Revised: 1 August 2018 | Accepted: 11 September 2018

DOI: 10.1002/qua.25817

WILEY International Journal of QUANTUM CHEMISTRY

FULL PAPER

Neutral and zwitterionic dopamine species adsorbed on silver surfaces: A DFT investigation of interaction mechanism

Ana C. Rossi-Fernández | Lorena A. Meier | Norberto J. Castellani

IFISUR, Universidad Nacional del Sur, CONICET, Departamento de Fisica, Bahía Blanca, Argentina

Correspondence
Norberto J. Castellani, IFISUR, Universidad Nacional del Sur, CONICET, Departamento de Fisica, Av. L. N. Alem 1253, B8000CPB - Bahía Blanca, Argentina.
Email: castella@criba.edu.ar

Funding information
Agencia Nacional de Promoción Científica y Tecnológica, Grant/Award Number: PICT-2014-1778; Consejo Nacional de Investigaciones Científicas y Técnicas; Universidad Nacional del Sur, Grant/Award Number: PGI 24/F063

Abstract

Biomolecules nondissociative adsorption on noble metals is a key process in metallic biosensors implying several questions related to the stability and orientation of such molecules. Here, the neurotransmitter dopamine (DA) adsorption on silver surface is investigated in the context of density functional theory (DFT). Two different dopamine isomers, the neutral (NDA) and zwitterionic (ZDA) species, and two different silver surfaces, Ag (110) and Ag(111), were considered. NDA shows relatively large binding energies, compared to previously studied π-π bonded systems. ZDA adsorbs even much more strongly although this species is less stable than NDA in vacuum. To elucidate the nature of the interaction between adsorbate and substrate, an electronic structure analysis was performed. Adsorbed NDA species suffers the loss of electronic charge, accompanied by a downshift of its molecular levels and the appearance of an attractive interaction of coulombic nature between adsorbate and substrate. The significant ZDA binding can be related to larger electron transfer and coupling between ZDA and Ag orbitals. Moreover, for both species, an important contribution of attractive noncovalent interactions of different degrees can be observed. The Ag substrate produces several modifications on NDA and ZDA vibrational frequencies. Noticeably relevant are the large red/blue shifts undergone by the N-H/O-H stretching bands of zwitterionic species, of up to −670/+430 cm^{-1}.

KEYWORDS

adsorption, Ag, density functional theory, neutral dopamine, silver, VASP, zwitterionic dopamine

1 | INTRODUCTION

Dopamine (DA) is a catecholamine that binds and activates cell surface receptors in humans and mammalians.[1] This neurotransmitter plays an important physiological role in the central nervous, renal, and hormonal systems.[2] Low or high levels of dopamine are related to serious human neural diseases, such as the Parkinson's disease and schizophrenia, respectively.[3] Therefore, it is of great medical and pharmacological interest to study chemical interactions in which this molecule is involved. According to the pD value of the solvent medium, different forms of catecholamine molecules have been reported, including neutral, zwitterionic, cationic, and anionic species.[4] Acid dissociation constants obtained from nuclear magnetic resonance data showed that cationic and anionic species predominate at acidic (pD < 7) and alkaline media (pD > 12), respectively, while at intermediate pD values the four species including neutral and zwitterionic are present.[4]

Recently, several proposals for DA detection have been published based on field effect transistor probes,[5] electrochemical[6] and optical techniques.[7–9] Regarding the latter technique, the most powerful is the surface-enhanced Raman spectroscopy (SERS), where a huge enhancement of adsorbed molecules Raman scattering is produced due to the resonance effect from surface plasmon modes in noble metals rough surfaces and nanoparticles (20-40 nm in size).[10] This spectroscopy has been widely used for biomolecules detection, to the point of confirming the single molecule nature of an observed signal.[11] SERS results reported by Bu and Lee[8] for DA anchored on Au, Ag, and $Ag_{core}Au_{shell}$ nanoparticles (NPs) showed that Au NPs exhibited higher sensitivity in the SERS detection of DA molecules at low concentrations, while Ag NPs displayed

stronger Raman intensity at high concentrations of DA. Subsequently, the same authors studied the optical properties of Ag NPs with adsorbed DA molecules as a function of pH, concluding that the Ag NPs clustering due to DA bridges between Ag NPs showed the maximal SERS activity to DA molecules in a limited pH range (pH = 7-9).[12] In a recent work related to the detection of DA with colorimetric probes based on Au NPs, the NPs cross-linking aggregation was attributed to the formation of hydrogen bonding between DA molecules anchored on Au NPs.[13] Conversely, the interplay of DA and Au NPs coated with Ag has been investigated in an earlier work by means of SERS and complemented with Fourier transform infrared and normal Raman spectroscopy results,[14] suggesting that the DA molecules are adsorbed onto $Au_{core}Ag_{shell}$ surface with the molecular plane tilted with respect to the silver surface. In relation to these experimental results, several open questions cannot be easily answered without a full description at the molecular level; namely, those related to adsorbed molecule geometrical orientation, adsorption sites coordination number, electron transfers to/from the surface, and competition between different adsorbed DA species.

Molecules adsorption on solid surfaces is a key process in various fields, including heterogeneous catalysis,[15] electrochemistry,[16] molecular sensing,[17,18] and minerals processing.[19,20] The understanding of physical and chemical properties involved in such process has benefited from theoretical chemistry. This was largely evident from the advent of density functional theory (DFT) methods, which permits to study molecules binding on metallic,[21,22] covalent[23] and ionic solid surfaces[24,25] with the same tool. So far, the study of biomolecules adsorption on noble metal surfaces has focused on the anchoring of nucleobases,[26] aminoacids,[27] and short[28] and very long peptides[29] in connection with DNA fragments identification and the formation of self-assembled molecular overlayers. However, the DA species adsorption on extended noble metal surfaces has not been studied theoretically before. We can mention a related study where both the neutral-DA-Ag_2 and zwitterionic DA-Ag_2 complexes were studied by means of DFT,[14] particularly focusing on the vibrational spectra of such species. Besides the relevance of a theoretical approach to the DA/Ag or analogous systems for a full comprehension and analysis of experimental results, the theoretical characterization of DA bonding with a noble metal surface is of major interest to verify earlier ideas about the interplay between complex organic molecules and late transition metals surfaces.

In the present approach neutral and zwitterionic DA species adsorption on the (110) and (111) Ag faces is theoretically investigated within the framework of DFT, representing the substrate with a periodic model. The case of zwitterionic DA is particularly noticeable due to the comparatively large energy gain produced when this molecule anchors onto the Ag surfaces. The resulting DA-silver interactions were elucidated by analyzing several aspects of the electronic structure of molecule/substrate systems, including charge transfers, molecular orbital coupling, and noncovalent index. It is worth mentioning that no other theoretical account for the adsorption of DA or other cathecolamine on extended metallic surfaces has previously been published.

2 | THEORETICAL METHOD

The results reported in this work are based on the DFT formalism and were implemented by means of the Vienna Ab initio Simulation Program (VASP).[30,31] In this code, the Kohn–Sham equations are solved employing a plane-wave basis and periodic boundary conditions. Electron exchange and correlation effects are described by the generalized gradient approximation using the functional due to Perdew–Burke–Ernzerhof.[32] The electron-ion interactions are taken into account by the projector-augmented wave (PAW) potentials. The PAW method is a frozen core all-electron method that uses the exact shape of the valence wavefunctions instead of pseudo-wavefunctions.[33,34] The $4d^{10}5s^1$ electronic configuration for external electrons was considered for Ag atoms. Taking into account that colloid noble metal nanoparticles exhibit mostly (111) planes and in a less proportion (200), (220), and (331) planes,[35,36] the Ag(111) and Ag(110) surfaces were selected for the present work. The latter is topographically very similar to Ag(220). Conversely, the atom arrows of Ag(110) surface can be considered as a model to mimic the edges effect in small cuboctahedral and icosahedral noble metal particles.[37] The repeated slabs representing the Ag(110) and Ag(111) surfaces contain five and four layers of atoms, respectively, and a vacuum gap in the normal direction. This gap width (14 Å) was optimized to minimize the interaction between slabs. The Ag(110) array has a 3 x 4 supercell with 60 silver atoms and the Ag(111) array has a 4 x 4 supercell with 64 silver atoms. All calculations were performed at the nonspin polarized level. Previous results for the Sn atoms adsorption on Au—a nonmagnetic noble metal as Ag[38]—showed that the spin polarized results are very similar to those at the nonspin polarized level. For the present work, test calculations were performed for doublet states, giving total electronic energies that are 0.01-0.02 eV less stable than the respective single states. The fixed convergence of the plane-wave expansion was obtained with 415 eV cutoff energy. Integrations in the first Brillouin zone were made using Monkhorst grids of 2 x 2 x 1 *k*-points. Nonlocal dispersive effects were included by using the DFT-D2 method due to Grimme´s group.[39]

The adsorption of neutral dopamine and its zwitterionic dopamine species, designated shortly as NDA and ZDA, respectively, was studied on both Ag(110) and Ag(111) surfaces. The interaction energy between one of these molecules and each Ag surface was calculated in terms of the adsorption energy, E_{ads}, defined as

$$E_{ads} = E_{adsorbate/substrate} - E_{substrate} - E_{adsorbate} \quad (1)$$

In this expression, $E_{adsorbate/substrate}$ is the total energy of NDA/Ag or ZDA/Ag systems, $E_{substrate}$ the total energy of the Ag substrate and $E_{adsorbate}$ the total energy of the NDA or ZDA molecule, respectively.

The adsorbed species and the first and second atomic layers for Ag(110) were allowed to relax until the residual Hellmann–Feynman forces were below 0.02 eV/Å. In the case of the Ag(111) surface, the adsorbed species and only the first atomic layer of the substrate were relaxed. The vibrational frequencies of isolated and the adsorbed NDA and ZDA molecules were calculated by diagonalizing the Hessian matrix as

implemented in VASP, considering a finite difference approach with a step size of 0.024 Å for the adsorbed atom displacement along each Cartesian coordinate. For the isolated NDA and ZDA dopamine species, additional calculations were carried out with the Gaussian 03 code at the B3LYP/6-31G theory level.[40]

The electronic structure was analyzed by computing the projected density of electronic states (PDOS) of specific adsorbate and substrate atomic states using a 7 x 7 x 1 *k*-points grid. The analysis of charge reorganization due to adsorption was accomplished by calculating the electronic charge density difference, $\Delta\rho$, produced as a consequence of the adsorption process. This electronic property can be expressed as

$$\Delta\rho = \rho_{\text{adsorbate/substrate}} - \rho_{\text{subsbtrate}} - \rho_{\text{adsorbate}} \tag{2}$$

where $\rho_{\text{adsorbate/substrate}}$ is the charge density of the total NDA/Ag or ZDA/Ag systems, $\rho_{\text{substrate}}$ the charge density of the Ag substrate, and $\rho_{\text{adsorbate}}$ the density of the NDA or ZDA molecule, the last two charge densities calculated as isolated fragments, but with the same geometry as for the adsorbed molecule on Ag. The charge of each fragment, NDA or ZDA molecule and Ag substrate, was evaluated performing a DDEC6 atomic-charge analysis.[41] This is an atoms-in-materials method where exactly one electron distribution is assigned to each atom, core electrons are assigned to the correct host atom, and net atomic charges are formally independent of the basis set type because they are functionals of the total electron distribution. The noncovalent interactions between adsorbate and substrate were analyzed by means of the NonCovalent Index (NCI),[42] as implemented in the last version of Critic code.[43] The NCI index is based on a 2D plot of the reduced density gradient, *s*, and the electron density, ρ, where

$$s = \frac{1}{2(3\pi^2)^{1/3}} \frac{|\nabla\rho|}{\rho^{4/3}} \tag{3}$$

If noncovalent interactions are present in a system, steep peaks appear at low density in this 2D plot. On one hand, the sign of λ_2, the second largest eigenvalue of the electron-density Hessian matrix, allows us to know the nature of this interaction and on the other hand, the electron density, the interaction strength. Then, the 3D plotting of sign(λ_2)ρ on an isosurface of the reduced density gradient renders possible defining regions of different noncovalent nature. The plotting of 3D isosurfaces for $\Delta\rho$ function was performed employing the VESTA3 code[44] and that for NCI index by the VMD code.[45] Vibrational normal modes visualization was performed employing the Jmol code.[46]

3 | RESULTS AND DISCUSSION

3.1 | The free neutral dopamine and zwitterionic dopamine species

The main geometrical parameters of DA neutral and zwitterionic forms have been evaluated taking into account the free molecule species as a reference for the adsorbed forms detailed in subsequent sections. Figure 1 shows the optimized geometries schemes for free dopamine species considered in the present work.

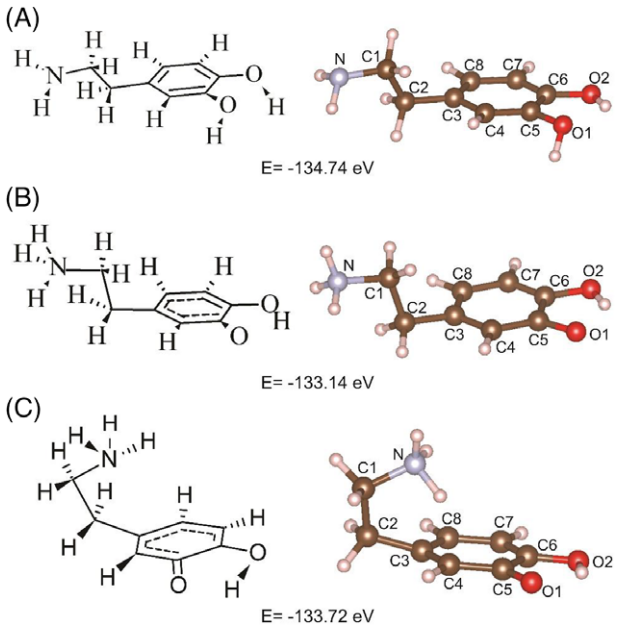

FIGURE 1 Schemes of the optimized geometries for free dopamine species considered: A, trans-conformer of neutral dopamine, NDA, B, trans-conformer of zwitterionic dopamine, ZDA, and C, gauche-conformer of zwitterionic dopamine, G-ZDA. Carbon atoms: Brown balls, oxygen atoms: Red balls, nitrogen atom: Light blue ball, hydrogen atoms: Small white balls. The total electronic energy value has been reported at the foot of each scheme

The DA molecule neutral form, whose semistructural formula is $C_6H_3(OH)_2$-CH_2-CH_2-NH_2, shows conformational isomerism owing to the presence of several internal rotation axes. In particular, taking into account the rotation around the C2-C1 axis, the isomer shown in Figure 1 for NDA corresponds to a trans-conformer, with the C3-C2-C1-N dihedral angle nearly zero. The other possibility, with this angle having $\pm 180^\circ$, gives a gauche-conformer. These two isomers differ by 0.05 eV or less.[47,48] The dopamine zwitterionic form, whose semistructural formula is $C_6H_3O(OH)$-CH_2-CH_2-NH_3, can show both conformational isomerism and configurational isomerism because of the substituents positions on the aromatic ring. More specifically, the OH group can be in metha or para-position with respect to the CH_2-CH_2-NH_3 group. The isomer shown in panel (b) of Figure 1 for ZDA corresponds to a trans-conformer, with the OH in para-position. Earlier calculations for the zwitterionic form of DA indicate that this isomer is more stable (by less than 0.01 eV) than the case with the OH in metha-position.[47,48] ZDA gauche-conformer reactivity will be considered particularly in section 3.3.

Table S1 in Supporting Information shows the most relevant interatomic distances and bonding angles for the NH_n and CH_2NH_n (n = 2, 3) groups obtained after geometry optimization with the VASP code. The corresponding total electronic energies for NDA and ZDA have been also reported in Figure 1. Notice that free NDA is 1.016 eV more stable than free ZDA, in agreement with previous calculations,[48] where the difference between respective ground states is even larger, about 2.3 eV. These results are compared in the same Supporting Information Table S1 with those obtained with the G03 code, as well as with the experimental data available from XRD experiments for dopamine hydrochloride, where dopamine adopts a cationic DA^+ form.[49] The interatomic distances values for NDA and ZDA differ by less than 0.01 Å mostly, comparing both theoretical methods. The bond angles considered differ by a mean of 0.9°. The dihedral angle C4-C3-C2-C1 which accounts the rotation of amine group with respect the aromatic plane differs by a mean of 1.7°. The comparison with the geometric parameters obtained from XRD data from Ref. [49] indicates that the experimental N-C1 and C1-C2 distances are longer and shorter than the theoretical ones obtained for NDA with VASP, respectively, by about 0.5 Å. The other distances agree by about 0.2 Å. Conversely, the value of experimental N-C1 and C5-C6 distances for ZDA is shorter and the C5-O1 distance longer than the theoretical value, by about 0.6 Å. The other distances agree by about 0.2 Å. Therefore, we note that a very reasonable NDA and ZDA geometries description can be attained using the VASP code which is consistent with both a molecular orbital method based on a localized basis set as G03 and the available experimental DA molecule data.

3.2 | Neutral dopamine species adsorbed on Ag surfaces

3.2.1 | Energetic and geometric results of NDA/Ag system

The configurations schematized in Figure 2 were considered to study the NDA molecule adsorption on Ag(110) and Ag(111). In these stacking geometries, named as S-110-a and S-110-b for Ag(110) and S-111 for Ag(111), the NDA molecule is placed initially parallel to the silver surface. The axis passing through atoms C3 and C6 of DA ring, which will be designated as the NDA-longitudinal-axis, is oriented along the [100] and [−110] directions, in the case of S-110-a and S-110-b adsorption modes on the Ag(110) surface, respectively. Figure 2 schemes are those obtained after optimization, with the ethylamine group oriented toward the vacuum.

The adsorption energy values, computed as described in section 2, and the most relevant geometrical parameters are shown in Table 1. The corresponding total electronic energies and the most visualizable heights of NDA atoms have also been reported in Figure 2. Notice that for all the geometries studied the adsorption is an exothermic process. The E_{ads} magnitude is in the 1.27-1.51 eV range and different adsorption sites follow the S-111 > S-110-b > S-110-a stability order. The remark that the (111) surface is more favorable than the (110) one can be related to the larger coordination number of exposed Ag atoms. The h_{C3} height, which can be taken as a measure of the distance between the NDA aromatic ring and the Ag surface, is in the 2.5-2.9 Å range and follows the S-111 > S-110-a > S-110-b height order. These values can be compared

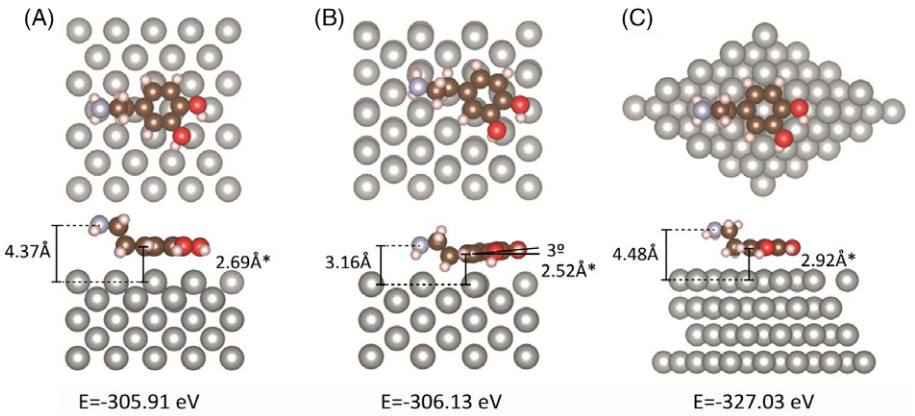

FIGURE 2 Optimized geometries for NDA/Ag(110) and NDA/Ag(111) systems: A, NDA/Ag(110) S-110-a mode, B, NDA/Ag(110) S-110-b mode, C, NDA/Ag(111) S-111 mode. Top and lateral views are shown. Silver atoms: Gray balls, carbon atoms: Brown balls, oxygen atoms: Red balls, nitrogen atom: Light blue ball, hydrogen atoms: Small white balls. The most visualizable heights of NDA atoms measured from the Ag first layer are included. The asterisk (*) corresponds to the height of C3 atom. The total electronic energy value has been reported at the foot of each system

to those corresponding to the adsorption of a molecule with aromatic structure and an amino-like substituent such as *NN*-dimethylaniline adsorbed on Ag(111)[50] where an E_{ads} value of −1.15 eV and a molecule-surface distance of 2.87 Å were obtained for a stacking configuration. In another comparison, the aromatic nucleobase adenine adsorbed on Ag(110) exhibits an E_{ads} value of −0.32 eV and a molecule-surface distance of 2.57-2.63 Å also for a stacking configuration.[51]

The O1 and O2 atoms heights (h_{O1} and h_{O2}, respectively) are both in the range 2.6-2.9 Å for the three adsorption modes. Conversely, the N atom height (h_N) and that of the hydrogen atom pertaining to O1-H hydroxyl group (h_{H1}) for the S-110-b mode are up to 1.2 Å and 0.6 Å smaller, respectively, than the values for the S-110-a and S-111 sites. The h_N value for the S-110-b mode can be related to a tilt of about 3° undergone by the NDA-longitudinal-axis which carries the ethylamine group toward the Ag surface. Besides, the fact that the S-110-b adsorption mode is more favored than the S-110-a is congruent with a lower h_{C3} height. The shortest interatomic distances between adsorbate and substrate atoms are for H-Ag (with H atom of methylene group of ethylamine substituent), C4-Ag, and H-Ag (with H atom of hydroxyl group in metha-position) bonds for S-110-a, S-110-b, and S-111 sites, respectively. They are 0.62, 0.28, and 0.77 Å larger than the respective sum of covalent radii. Concerning the adsorbed NDA internal angles, their values have also been summarized in Table 1, while the internal bonds have been reported in Figure S1 of Supporting Information. In both cases, they are compared with the values for the free NDA molecule. We can observe that there are only minor changes in NDA bond distances and the N-C1-C2 bond angle when this dopamine species is adsorbed on Ag. Conversely, a significant change can be observed in the C4-C3-C2-C1 dihedral angle which decreases 14.7% in the S-110-b mode, in comparison to the other modes with changes smaller than 5% in magnitude.

With the aim to analyze the effect of adsorption process on the adsorbate and substrate geometries, we can define the deformation energies for adsorbate and substrate fragments, $E_{def/adsorbate}$ and $E_{def/\ substrate}$, respectively, as:

$$E_{def/adsorbate} = E_{adsorbate^*} - E_{adsorbate} \tag{4}$$

and

$$E_{def/substrate} = E_{substrate^*} - E_{substrate} \tag{5}$$

where $E_{adsorbate^*}$ and $E_{substrate^*}$ account for the total energy of these fragments as free species, but with the geometries relaxed to the geometry of the adsorbate/substrate system. The corresponding computed values are summarized in Table 1. We can observe that the total amount of energy required to adapt the fragments to the adsorbed state can reach to 27% of the E_{ads} magnitude. In particular for the S-110-a mode, the energy required by Ag substrate deformation—about 20% of $|E_{ads}|$—is much larger than that required by NDA molecule deformation. They are of similar magnitude for S-110-b—10–17% of $|E_{ads}|$—while for S-111 mode, both deformation energies are less than the 3% of $|E_{ads}|$. The S-110-b mode result can be associated with the above-commented tilt of about 3° undergone by the NDA-longitudinal-axis. NDA behavior on Ag(110) contrasts to that obtained earlier for adenine on Ag(110), where $E_{def/adsorbate}$ is much more significant than $E_{def/substrate}$. However, the $E_{def/adsorbate}$

TABLE 1 Calculated parameters for NDA/Ag(110) and NDA/Ag(111) systems and different adsorption modes considered

	NDA/Ag(110)		NDA/Ag(111)
	S-110-a	S-110-b	S-111
E_{ads} (eV)	−1.272	−1.489	−1.515
$E_{ads/VDW}$ (eV)	−1.591	−1.990	−1.735
$E_{ads/GGA}$ (eV)	0.319	0.510	0.220
$E_{def/NDA}$ (eV)	0.037	0.155	0.046
$E_{def/Ag}$ (eV)	0.262	0.254	0.019
h_N (Å)	4.37	3.16	4.48
h_{C3} (Å)	2.69	2.52	2.92
h_{O1} (Å)	2.76	2.64	2.96
h_{O2} (Å)	2.65	2.82	2.94
h_{H1} (Å)[a]	2.41	1.84	2.37
N-C1-C2 (°) (115.41)[b]	115.34	114.01	114.79
C4-C3-C2-C1 (°) (86.98)[b]	87.95	74.17	91.32
Q_{NDA}(e)	0.237	0.224	0.168
Q_{Ag}(e)	−0.237	−0.224	−0.168

[a] H1 corresponds to the H atom of O1H hydroxyl group.
[b] Between brackets, the value for free NDA.
Energetic parameters: Adsorption energy (E_{ads}), vdW contribution to E_{ads} ($E_{ads/VDW}$), standard exchange and correlation contribution to E_{ads} ($E_{ads/GGA}$), adsorbate deformation energy ($E_{def/adsorbate}$), substrate deformation energy ($E_{def/substrate}$); main geometrical parameters: NDA atoms heights measured from the Ag first layer, bond and dihedral angles of NDA; fragment charges of NDA (Q_{NDA}) and substrate (Q_{Ag}).

values for adenine on Ag(110)[51] and DNA nucleosides on Au(100),[52] which are up to 10% and 20% of $|E_{ads}|$, respectively, can be considered analogous to our results.

The contribution of vdW-like dispersive interactions to the adsorption energy can be evaluated by DFT-D2 method. This contribution is designated in Table 1 as $E_{ads/VDW}$. The non-vdW contribution from the standard exchange and correlation interactions is named as $E_{ads/GGA}$. From the values summarized in Table 1, we can observe that the first contribution is in the range of −1.59 to −1.99 eV, while the second contribution is in the range of 0.22 to 0.51 eV for the three adsorption sites considered. Therefore, the electronic contribution is repulsive and NDA to Ag binding is mainly due to attractive dispersive interactions. This remark was outlined before for NDA adsorption on graphene[53] and for adenine on graphene,[54] which was attributed to the fact that at adsorbate-substrate distances less than 3 Å, the kinetic energy contribution to the energy of single-particle Kohn–Sham orbitals is more relevant than the attractive contribution due to electronic exchange and correlation effects. Conversely, the presence of attractive interactions in the non-vdW contribution cannot be discarded for the NDA/Ag system, as it was explained for the case of adenine adsorption on Cu(110), where the binding was attributed to an ionic interaction between adsorbate and substrate.[55] Besides, an interesting comparison can be made between the results for adsorption modes S-110-a and S-111. Notice that the larger E_{ads} magnitude for the second site is obtained as a consequence of the concertation of a smaller magnitude (by 0.25 eV) of $E_{ads/VDW}$, an attractive term, and an even smaller magnitude (by 0.29 eV) of $E_{ads/GGA}$, a repulsive term. The two last facts can be related with the higher (by 0.1-0.4 Å) values for h_{C1}, h_{O1}, and h_{O2} heights obtained for the S-111 mode.

3.2.2 | Electronic structure analysis of NDA/Ag system

For the purpose of studying a possible charge transfer between adsorbate and substrate, the electronic charge density difference, $\Delta\rho$, of the NDA/Ag system was calculated with respect to the isolated fragments constituted by the NDA molecule and the Ag substrate. Figure 3 shows the $\Delta\rho$ distribution corresponding to the three adsorption sites considered. We can notice that an electron charge density redistribution takes place with an increase (blue color) in the region near to the substrate first plane and a decrease (red color) in the region occupied by the NDA molecule. To quantify this effect a DDEC6 atomic-charge analysis was performed.[41] The net charge corresponding to the NDA and Ag fragments of a unit cell are summarized in Table 1. We can observe that an electron charge transfer of 0.17-0.24e takes place from the NDA molecule to the Ag surface, in agreement with the results for $\Delta\rho$, allowing the formation of some attractive ionic interaction between adsorbate and substrate. A similar observation was reported for the adenine adsorption on Ag(110)[51] and *NN*-dimethylaniline on Ag(111).[50] In the latter system, the availability of an aromatic ring to give electron charge was related to the fact that the $N(CH_3)_2$ group is a strong activating substituent of benzene. In the case of NDA, the ethylamine group acts at least as a medium strength activating substituent of the NDA aromatic ring.

To analyze the electronic structure inherent to the NDA/Ag system, we proceeded to calculate the PDOS on specific unit cell fragments. Figure 4 shows the PDOS on NDA and the first layer of Ag(110). Two scenarios are compared; namely, NDA placed far apart from Ag(110) surface; that is, in a situation with quasi no interaction between adsorbate and substrate, and NDA adsorbed on Ag(110) in the S-110-a mode. On NDA adsorption the main PDOS constituent on the first layer of Ag(110), that is, the Ag d-band, does not show any appreciable modification on its profile. Therefore, we can expect that no relevant coupling is established between the Ag d-orbitals and NDA atomic orbitals and that no evident covalent interactions are present between adsorbate and substrate. Conversely, the different peaks corresponding to occupied NDA molecular orbitals move to greater binding energies. Indeed, the selected NDA levels designed as (i) and (ii) in Figure 4 show a shift from −0.70 to −0.74 eV to lower energies measured with respect to the Fermi level. This result can be rationalized with the presence of a positive charged region on the NDA molecule that stabilizes NDA energy levels and correlates with the above comment of an electron charge transfer from adsorbate to substrate.

NCI analysis was performed for this system taking into account the role noncovalent interactions could play on NDA/Ag. Figure 5 shows the 2D NCI-plots for NDA/Ag in the S-110-b and S-111 adsorption modes, calculated with the charge density coming from the DFT-D2 method. The appearance of a steep peak for negative and near zero values of $\text{sign}(\lambda_2)\rho$ as well as a bulky peak around −0.025 a.u. are evidence for the presence of attractive interactions of noncovalent nature. While the steep peak is more proper of van der Waals interactions, the second supports the

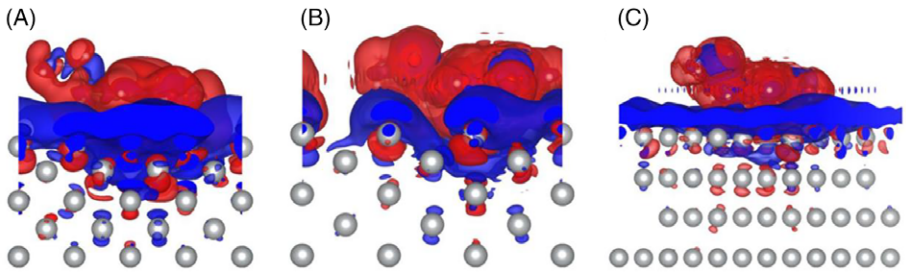

FIGURE 3 Charge density difference ($\Delta\rho$) plots for NDA adsorbed on Ag: A, NDA/Ag(110) S-110-a mode, B, NDA/Ag(110) S-110-b mode, C, NDA/Ag(111) S-111 mode. Isosurfaces corresponding to $\Delta\rho = \pm 8.10^{-5}$ bhor^{-3} are depicted. Blue regions show electron charge accumulation; red regions, electron charge loss. Ball colors for atoms as in Figure 2

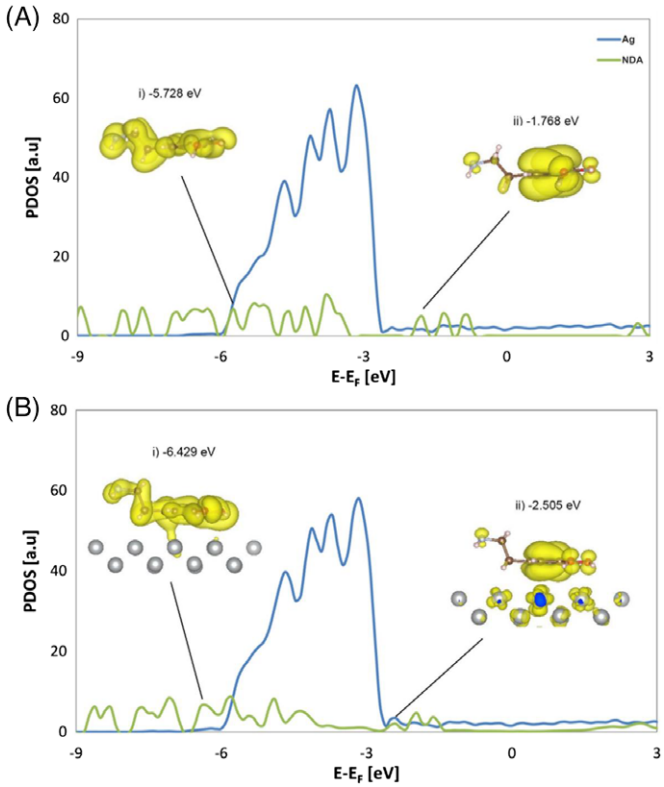

FIGURE 4 Electronic projected-DOS on the NDA molecule (NDA) and on the first Ag layer (Ag) of NDA/Ag(110) system: A, NDA molecule placed far from Ag(110), B, NDA molecule adsorbed on Ag(110) in S-110-a mode. The insets (i), on the left, and (ii), on the right, display the electronic charge density (ρ) isosurfaces (5.10^{-5} bhor^{-3}) for selected levels of NDA, respectively. The corresponding energy eigenvalues are also indicated. The calculations of ρ were performed at the Γpoint

formation of stronger bonding.[43] Nevertheless, part of this feature comes from noncovalent interactions established between Ag atoms, as it is shown in the NCI analysis of naked Ag substrate displayed in Figure S3 of Supporting Information.

Looking at the 3D plot for negative values of λ_2 displayed in Figure 5 for the case of NDA adsorbed in the S-110-b mode of Ag(110) surface, we note the presence of green color regions associated with van der Waals interactions and light blue color ones associated to the aforementioned stronger noncovalent interactions. Conversely, the regions associated with van der Waals interactions are less defined and smaller in size

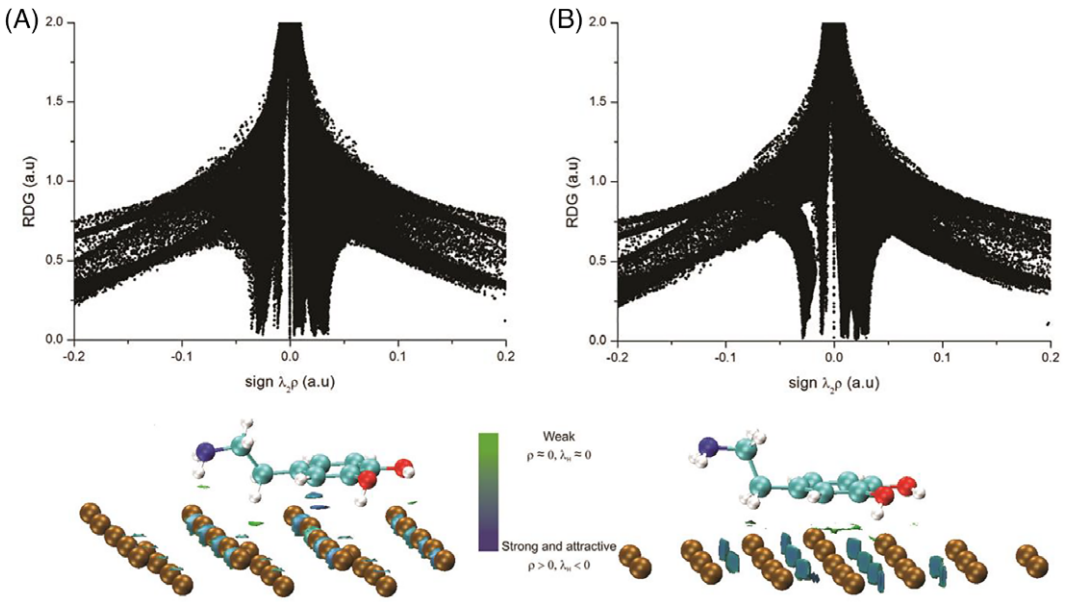

FIGURE 5 2D (left panel) and 3D (right panel, perspective view) NCI plots for NDA adsorbed on Ag: A, NDA/Ag(110) S-110-b mode, B, NDA/Ag (111) S-111 mode. 3D NCI isosurfaces correspond to s = 0.25 and a color scale of $-0.1 \leq \text{sign}(\lambda_2)\rho \leq 0$ bhor^{-3}

for the case of NDA adsorbed in the S-111 mode of Ag(111) surface, this observation being in agreement with the above comment on the comparative smaller $E_{ads/VDW}$ magnitude.

3.2.3 | General discussion on the NDA/Ag system

From the above results we notice that there is a straight correlation between the Ag surface coordination number and DA adsorption energy magnitude; the more compact exposed plain (111) showing the largest value. Conversely, for DA adsorbed on the (110) plane, there is also a dependence on the DA molecule orientation along the surface; the [−110] direction being the most favored. In the latter case—the S-110-b mode—the internal C4-C3-C2-C1 dihedral angle suffers an important distortion. Compared with other aromatic molecules adsorbed on noble metals, the adsorption energy magnitude is larger while the distance of aromatic ring to the surface plane is similar. The interatomic distances between the adsorbate and substrate are compatible with the presence of noncovalent interactions; therefore, in principle, it can be argued that a large part of the binding comes from this source. The analysis accomplished on different energy contributions and on electronic structure properties allowed us to quantify and identify the different contributions. Indeed, E_{VDW} contribution is essential to define the stability on the three surfaces considered. Nevertheless, besides the large charge redistribution, a net electron transfer is produced from DA to Ag, causing a shift in DA levels. Therefore, an ionic interaction is also present which counteracts partially the repulsive contributions to E_{GGA} due to DA closed valence shells. Conversely, the noncovalent interactions of dispersive nature can be localized mainly between the aromatic ring and Ag substrate atoms, rather than between the ethylamine group and Ag substrate atoms.

3.3 | Zwitterionic dopamine species adsorbed on Ag surfaces

3.3.1 | Energetic and geometric results of ZDA/Ag system

With the aim to study the ZDA molecule adsorption on Ag(110) and Ag(111), the configurations schematized in Figures 6 and 7 were considered, respectively. These figures schemes were obtained after optimization for each of the adsorption modes. As the zwitterionic DA species is a dipolar ion, we were interested in studying adsorption configurations where both dipoles are near the Ag surface and those where only one of the ZDA electric charges, positive or negative, is near the substrate. In the stacking configurations named as S-110-a and S-110-b for Ag(110) and S-111 for Ag(111), the ZDA molecule is placed initially parallel to the silver surface. They are similar to the stacking configurations for the neutral DA species. In the perpendicular configurations, the axis passing through the ethylamine group of ZDA ring and the hydroxyl group in para-position of this same ring, which will be designated by ZDA-longitudinal-axis, is oriented initially normally to the Ag surface. There are two perpendicular orientations, perpendicular-ethylamine (ea) and perpendicular-hydroxyl (oh). In the first case, the ethylamine group is oriented toward the Ag surface, whereas in the second case, the hydroxyl group is oriented toward the surface. These orientations are named P-110-ea and P-110-oh, respectively, for Ag(110) and P-111-ea and P-111-oh, respectively, for Ag(111). Figure 7 shows that the ZDA hydroxyl group adopts finally a metha-position with respect to the amino group in the case of the P-111-oh mode, unlike other adsorption modes where the initial para-position is preserved.

Adsorption energy values computed as described in section 2 and the most relevant geometrical parameters are shown in Table 2. The corresponding total electronic energies and the most visualizable ZDA atoms heights have also been reported in Figures 6 and 7. We highlight that for all the geometries studied, the adsorption is an exothermic process. E_{ads} magnitude for the stacking modes is in the 2.76-3.08 eV range, that is, about 1.5 eV larger than the results for NDA adsorbed on the same sites. Moreover, these adsorption sites follow the S-111 > S-110-a > S-100-b stability order, similarly to NDA/Ag case, favoring the adsorption mode on the Ag(111) surface, where the exposed Ag atoms have larger

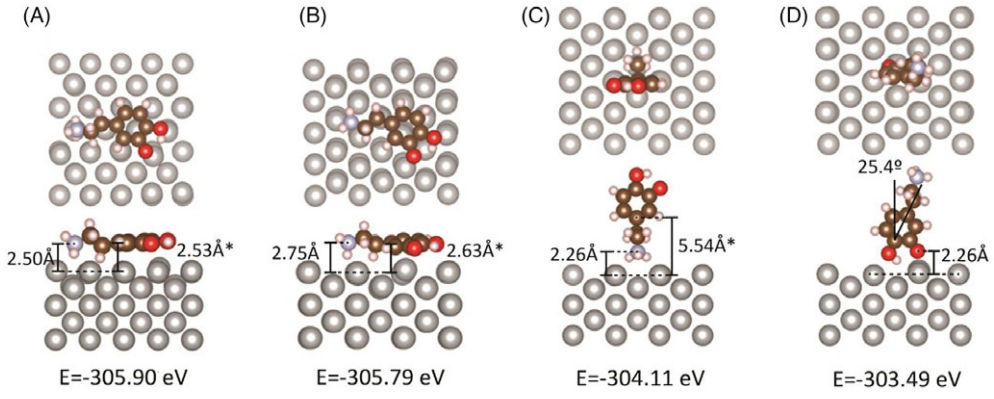

FIGURE 6 Optimized geometries for ZDA/Ag(110) system: A, ZDA/Ag(110) S-110-a mode, B, ZDA/Ag(110) S-110-b mode, C, ZDA/Ag(110) P-110-ea mode, D, ZDA/Ag(110) P-110-oh mode. Top and lateral views are shown. Silver atoms: Gray balls, carbon atoms: Brown balls, oxygen atoms: Red balls, nitrogen atom: Light blue ball, hydrogen atoms: Small white balls. The most visualizable heights of NDA atoms measured from the Ag first layer are included. The asterisk (*) corresponds to the height of C3 atom. The total electronic energy value has been reported at the foot of each system

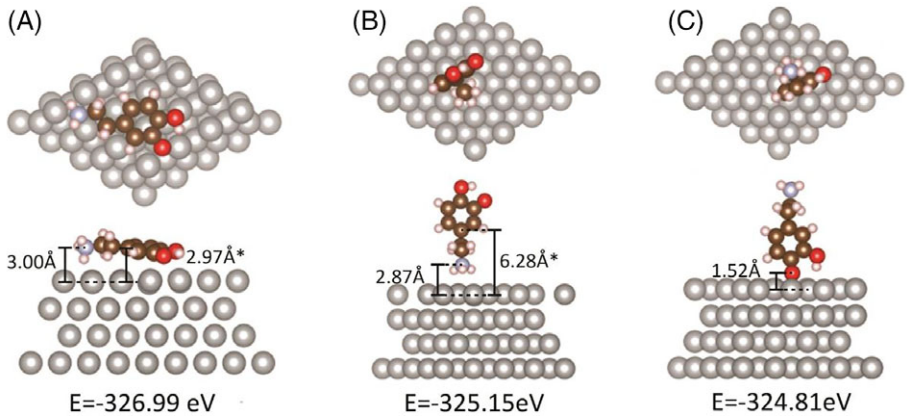

FIGURE 7 Optimized geometries for ZDA/Ag(111) system: A, ZDA/Ag(111) S-111-mode, B, ZDA/Ag(111) P-111-ea mode, C, ZDA/Ag(111) P-111-oh mode. Top and lateral views are shown. Silver atoms: Gray balls, carbon atoms: Brown balls, oxygen atoms: Red balls, nitrogen atom: Light blue ball, hydrogen atoms: Small white balls. The most visualizable heights of NDA atoms measured from the Ag first layer are included. The asterisk (*) corresponds to the height of C3 atom. The total electronic energy value has been reported at the foot of each system

coordination number than those of Ag(110) surface. It is noteworthy that compared with NDA, the highest ZDA reactivity against the Ag surface goes in the opposite direction to the relative stability of these dopamine species in the gas phase, where the NDA molecule is more favored by nearly 1 eV.

E_{ads} magnitude for perpendicular modes of adsorbed ZDA is in the 0.46-1.24 eV range, that is, about 2.1 eV smaller than the results for stacking sites. The corresponding P-111-ea > P-110-ea > P-111-oh > P-110-oh stability order shows that besides the favoring effect due to the coordination number of exposed Ag atoms, ZDA molecule prefers to link to Ag through the amino group instead of through the hydroxyl. This preference of ea-modes over oh-modes—by 0.3-0.6 eV—is in line with a recent experimental study concerning the detection of dopamine based on cross-linking Au nanoparticles aggregation[13] which would be induced by hydrogen bonding between dopamine molecules hydroxyls with a simultaneous dopamine molecule anchoring to the Au surface via amino groups.

The shortest interatomic distances between atoms of adsorbate and substrate for S-110-a, S-110-b, and S-111 sites are for the O1-Ag, O1-Ag, and H-Ag (with H atom of amino group of ethylamine substituent) bonds, respectively. They are 0.02, 0.06, and 0.44 Å larger than the respective sum of covalent radii. Besides, the O1-Ag bond of S-111 site is 0.26 Å larger. C3 atom height for the adsorbed ZDA stacking modes is in the 2.5-3.0 Å range and follows the S-111 > S-110-b > S-110-a height order. In this sense, the behavior of Ag(111) surface is analogous to that

TABLE 2 Calculated parameters for ZDA/Ag(110) and ZDA/Ag(111) systems and different adsorption modes considered

	ZDA/Ag(110)				ZDA/Ag(111)		
	S-110-a	S-110-b	P-110-ea	P-110-oh	S-111	P-111-ea	P-111-oh
E_{ads} (eV)	−2.860	−2.755	−1.075	−0.456	−3.080	−1.238	−0.899
$E_{ads/VDW}$ (eV)	−2.332	−2.350	−0.780	−1.106	−2.729	−0.524	−0.800
$E_{ads/GGA}$ (eV)	−0.528	−0.405	−0.295	0.701	−0.352	−0.714	0.099
$E_{def/ZDA}$ (eV)	0.088	0.219	0.632	0.751	0.050	0.652	0.841
$E_{def/Ag}$ (eV)	0.411	0.385	0.265	0.413	0.019	0.027	0.113
h_N (Å)	2.50	2.75	2.26	9.67	3.00	2.87	9.28
h_C (Å)[a]	2.52	2.63	5.54	3.22	2.97	6.28	2.84
h_O (Å)[b]	2.32	2.09	9.90	2.26	2.22	10.73	1.52
h_H (Å)[c]	2.76	2.67	1.73	1.38	2.65	2.38	2.12
C2-C1-N (°) (111.13)[d]	106.86	109.38	110.57	111.34	110.32	109.95	111.42
C4-C3-C2-C1 (°) (94.17)[d]	55.98	41.72	86.82	99.99	−171.46	88.68	83.54
Q_{ZDA} (e)	0.300	0.331	0.378	0.045	0.304	0.433	0.170
Q_{Ag} (e)	−0.300	−0.331	−0.378	−0.045	−0.304	−0.433	−0.170

[a] C3 carbon atom of ZDA ring for stacking and perpendicular-ea sites, C6 carbon atom for perpendicular-oh sites.
[b] O1 atom of ZDA for all sites, except the P-111-oh, where the O2 atom was considered.
[c] Hydrogen atom of ZDA nearest to the surface.
[d] Between brackets, the value for free ZDA.
Energetic parameters: Adsorption energy (E_{ads}), vdW contribution to E_{ads} ($E_{ads/VDW}$), standard exchange and correlation contribution to E_{ads} ($E_{ads/GGA}$), adsorbate deformation energy ($E_{def/adsorbate}$), substrate deformation energy ($E_{def/substrate}$); main geometrical parameters: ZDA atoms heights measured from the Ag first layer, bond and dihedral angles of ZDA; fragment charges of ZDA (Q_{ZDA}) and substrate (Q_{Ag}).

obtained for adsorbed NDA. Conversely, N atom height for all the stacking modes is 0.41-1.87 Å lower than that for the same sites of NDA/Ag system, indicating that the ZDA molecule becomes largely deformed in comparison with the NDA molecule because of a reorientation of ethylamine group, as it will be discussed later. Consequently, amino N atom and aromatic C3 atom heights are very similar (see Figures 6 and 7). Besides, note that O1 atom height for ZDA molecule adsorbed on S-110-b and S-111 sites is 0.7-0.8 Å lower than that of C3 atom. This observation can be associated to the fact that the ZDA ring exhibits noncoplanarity for this molecule adsorbed on S-110-b and S-111 sites. Two axes contained in the ZDA aromatic plane were considered to describe this geometrical remark. One is the above-described ZDA-longitudinal-axis passing through C3 and C6 atoms, and the other is an axis perpendicular to the former, passing through C5 and C7 atoms. Thus, we can see that the ZDA ring rotates clockwise by about 9° and 12° around the C3-C6 axis, for S-110-b and S-111 sites, respectively, compared with the S-110-a site, with a rotation of only 2°. Likewise, the ZDA ring plane rotates by about −11° around the other C5-C7 axis for the S-111 site, compared with S-110-a and S-110-b sites, where a counterclockwise rotation of 3°-4° was obtained.

The shortest interatomic distances between adsorbate and substrate atoms for P-110-ea and P-111-ea sites are for the H-Ag (with H atom of amino group of ethylamine substituent) bond, while for P-110-oh and P-111-oh sites, they are for the O1-Ag and O2-Ag bonds, respectively. They are 0.71, 0.70, 0.08, and 0.14 Å larger than the respective sum of covalent radii. N atom height of amino group for the P-110-ea mode is 0.61 Å lower than that for the P-111-ea mode because the former surface is more open, allowing a nearer approach of ZDA molecule to the surface. This is also valid when we compare the O1 atom heights for the P-110-oh and P-111-oh modes, the former being 0.79 Å lower than the latter; in addition, for P-111-oh, the hydroxyl change from para- to metha-position makes the O2 atom the nearest to the surface. ZDA adsorption in the P-110-oh mode on the Ag(110) surface exhibits a remarkably tilting of 25.4°, a not observed behavior in other perpendicular modes.

Table 2 summarizes the values of the internal adsorbed ZDA angles, while Figure S2 and Table S2 of Supporting Information report the internal bonds. In all cases, they are compared with the values for the free ZDA molecule. We can observe that the C-C bonds of the aromatic and those of ethylamine substituent show minor changes. The C5-O1 and C6-O2 bonds shorten by 2.3% in the perpendicular-ea sites, whereas they stretch up to 2.0% in perpendicular-oh sites. The C1-N bond is the most affected: it shortens up to 3.8% in the stacking and perpendicular-ea sites, but to a lower degree, 1.9%, in the perpendicular-oh sites. Systematically the O-H bond shortens by up to 0.03 Å and at least one N-H bond of ammonium group stretches by about 0.02 Å, for all adsorption configurations considered. Larger changes are suffered by the C4-C3-C2-C1 dihedral angle for the stacking modes. The phenylamine substituent undergoes a 38°-52° counterclockwise rotation for S-110-a and S-110-b, and a 94.37° clockwise rotation for S-111. As a consequence, in the last case the two methylene groups of phenylamine become placed approximately in the same plane corresponding to the ZDA aromatic ring. The C4-C3-C2-C1 dihedral angle for the perpendicular modes shows changes from −11.3 to 6.2% in magnitude. The modifications undergone by the N-C1-C2 bond angle are in general less than 1.6% in magnitude, except for the S-110-a site, where it decreases 3.8%.

An interesting question arises in relation to the reactivity of ZDA gauche-conformer versus that of the trans-conformer. In the gas phase, the former isomer becomes more stable than the latter.[48] In addition, the amine group is oriented toward the aromatic ring which could have an important influence on adsorption behavior. From now on, the ZDA gauche-conformer will be named as G-ZDA, whereas the trans-conformer will be identified ZDA, as previously named. In Figure 1, the scheme of the optimized geometry for free G-ZDA and its total electronic energy value are shown. Notice that using the DFT-D2 method the free G-ZDA conformer is 0.582 eV more stable than the free trans-conformer ZDA, in agreement with a previous result.[33] Table 3 summarizes the adsorption energy values, computed as described in section 2, those of the total electronic energy and the selected geometric parameters values for prominent G-ZDA adsorption modes. For the present discussion, the stacking S-110-a and S-111 and the perpendicular P-110-ea and P-111-ea modes were considered; in the latter two modes, the OH group is oriented toward the vacuum. For the sake of comparison, the same Table 3 also shows the corresponding values for adsorbed ZDA (trans-conformer). We can observe that in the case of stacking sites the E_{ads} magnitude for the G-ZDA isomer is 1-1.5 eV smaller than that for the ZDA isomer, while in the case of perpendicular sites, it is 0.5-0.6 eV smaller. The larger difference obtained for the former sites points out that the availability of amino group to interact with the Ag surface is an important factor to explain the higher reactivity of trans-conformer, at least in the case of stacking adsorption modes.

Notice that the total electronic energy of G-ZDA/Ag systems for the perpendicular sites is more negative than that of ZDA/Ag systems. Instead, the total electronic energy of ZDA/Ag systems becomes more negative for the stacking sites, in correspondence with the fact that for the latter sites the interaction between ZDA and Ag substrate is more significant than that between G-ZDA and Ag substrate. The N atom height is larger for G-ZDA/Ag systems, compared with ZDA/Ag, in agreement with the smaller E_{ads} magnitude. Conversely, the C3 atom of the aromatic ring for perpendicular-ea sites of G-ZDA/Ag system is nearer to the Ag surface due to the different amino group orientation with respect to this ring. The interatomic distance between H atom of the amino group and C4 atom in G-ZDA aromatic ring for the free species, 1.8 Å, indicates the formation of an intramolecular hydrogen bond; this bond weakens on adsorption, becoming stretched to 2-2.2 Å. The C4-C3-C2-C1 dihedral angle of G-ZDA distorts in -20° for the S-110-a adsorption mode and in the -3° to -8° range for the other modes. The C3-C2-C1-N dihedral angle of G-ZDA distorts in the 10° to 21° range.

The deformation energies $E_{def/adsorbate}$ and $E_{def/substrate}$ for ZDA/Ag systems are summarized in Table 2. We can observe that for the stacking modes the total amount of deformation energy can reach up to 22% of the E_{ads} magnitude, with a relative relevance for each contribution which is similar to that afore-attained for NDA/Ag. Conversely, the sum of these deformation energies can reach up to 55-83% of $|E_{ads}|$ for the perpendicular P-110-ea and P-111-ea modes, or be slightly larger (by a 1.06 factor) or much larger (by a 2.55 factor) than $|E_{ads}|$ for the P-110-oh and P-111-oh modes, respectively. Moreover, these energies can even represent a non-negligible fraction of the binding energy per atom for ZDA

TABLE 3 Calculated of G-ZDA/Ag(110) and G-ZDA/Ag(111) systems for most prominent adsorption modes of adsorbed G-ZDA (gauche-conformer)

	G-ZDA/Ag(110)		G-ZDA/Ag(111)	
	S-110-a	**P-110-ea**	**S-111**	**P-111-ea**
E_{ads} (eV)	−1.864 (−2.860)	−0.699 (−1.075)	−1.689 (−3.080)	−0.735 (−1.238)
$E_{adsorbate/substrate}$ (eV)	−305.486 (−305.900)	−304.321 (−304.115)	−326.185 (−326.994)	−325.232 (−25.152)
h_N (Å)	4.63 (2.50)	3.24 (2.26)	5.30 (3.00)	4.29 (2.87)
h_C (Å)[a]	3.04 (2.52)	4.26 (5.54)	2.76 (2.97)	4.52 (6.28)
h_H (Å)[b]	2.79 (2.76)	1.43 (1.73)	2.75 (4.43)	2.37 (2.38)
d_{CH} [1.84][c,d]	2.06	2.24	2.16	2.00
C4-C3-C2-C1 [59.96] (°)[d]	39.72 (55.98)	54.92 (86.82)	56.38 (−171.46)	51.75 (88.68)
C3-C2-C1-N [18.12] (°)[d]	39.38 (−169.30)	37.99 (−178.21)	33.33 (164.25)	27.89 (−176.75)

[a] Height of C3 atom of G-ZDA measured from the Ag first layer.
[b] Height of H atom of G-ZDA nearest to the surface, measured from the Ag first layer.
[c] Inter-atomic distance between H atom of amino group and C4 atom in G-ZDA aromatic ring.
[d] Between square brackets, the value for free G-ZDA.
Energetic parameters: Adsorption energy (E_{ads}), total electronic energy for adsorbate/substrate system ($E_{adsorbate/substrate}$); main geometrical parameters: G-ZDA atoms heights measured from the Ag first layer, internal G-ZDA C-H bond, G-ZDA dihedral angles. For comparison, the values for adsorbed ZDA (trans-conformer) are also shown between brackets.

molecule and of the cohesive energy per atom for Ag substrate. In other words, in the case of perpendicular modes both adsorbate and substrate are subject to a large strain due to the adsorption process. The origin of this behavior will be discussed later on.

$E_{ads/VDW}$ and $E_{ads/GGA}$ contributions to the adsorption energy for different ZDA/systems, computed according to Equations (4) and (5), are summarized in Table 2. We note that the van der Waals contribution is in the −2.33 to −2.73 eV range for the stacking modes and in the −0.52 to −1.11 eV range for the perpendicular ones. In particular the perpendicular-oh modes are about 0.3 eV more negative than the perpendicular-ea ones. The non-vdW contribution, $E_{ads/GGA}$, is negative (ie, attractive), in the −0.29 to −0.71 eV range, for the majority of sites except for the P-110-oh and P-111-oh sites, where this contribution is positive (ie, repulsive), in the 0.10 to 0.70 eV range. This behavior contrasts to that obtained for NDA/Ag, where a repulsive $E_{ads/GGA}$ contribution is present for the same adsorption modes. In addition, the E_{ads} larger magnitude for S-111 mode, compared with S-110-a and S-110-b modes, comes mainly from its larger $|E_{ads/VDW}|$ value, compensating the smaller $|E_{ads/GGA}|$ one.

3.3.2 | Electronic structure analysis of ZDA/Ag system

In Figure 8, the electronic charge density difference, $\Delta\rho$, of ZDA/Ag systems is displayed. Looking at the results for different modes, we note that a rearrangement of the electron charge density takes place, with an increase in the region near to the substrate first plane and a decrease in the region occupied by the ZDA molecule. This observation is similar to that outlined above for NDA/Ag systems, but more noticeable. The exceptions are the P-110-oh and P-111-oh sites, where these regions appear more mixed. The quantification of this effect is given in Table 2 where the net charge of ZDA and Ag fragments of a unit cell are summarized. They were computed according to the DDEC6 analysis.[41] We can see that in general an electron charge transfer of 0.30-0.43e from ZDA molecule to Ag surface is produced, except for the P-110-oh and P-111-oh sites, where the electron transfer is of 0.04-0.17e, respectively. Both observations are in agreement with the $\Delta\rho$ plots aforementioned and allow us to infer that an attractive ionic interaction between adsorbate and substrate is present in most of the adsorption modes. The transfer for ZDA adsorbed on stacking modes is 0.13-0.19e greater than that found for NDA/Ag. It is worth mentioning that according to the reasoning of Ref. [50] for *NN*-dimethylaniline adsorbed on Ag(111) and taking into account that the ethylammonium $(CH_2)_2NH_3$ group is a stronger activating benzene substituent than the ethylamine $(CH_2)_2NH_2$ group, a larger electron transfer should be expected to take place from ZDA to the substrate, compared with NDA.

In addition to this rearrangement of electron charge, an important Ag surface polarization should be expected when the NH_3^+ and O^--substituents of dipolar ZDA molecule are near to this Ag surface in the perpendicular adsorption modes. Indeed, the DDEC6 atomic charges of the three H atoms of NH_3^+ and their nearest Ag atoms for the perpendicular-ethylamine sites are in the 0.25 to 0.28e and −0.09 to −0.12e ranges, respectively (0.35e and 0.00e are the values for the respective separated fragments); and the DDEC6 atomic charges of the O^--substituent and its nearest Ag atoms for the perpendicular-hydroxyl sites are in the −0.40 to −0.43e and 0.08 to 0.15e ranges, respectively (−0.63e and 0.00e are the values for the respective separated fragments). To compute the electrostatic energy associated with these local polarized charges, $E_{elec/loc}$, we considered punctual charges centered on each atom. Although this way of calculation is a rather crude approximation to

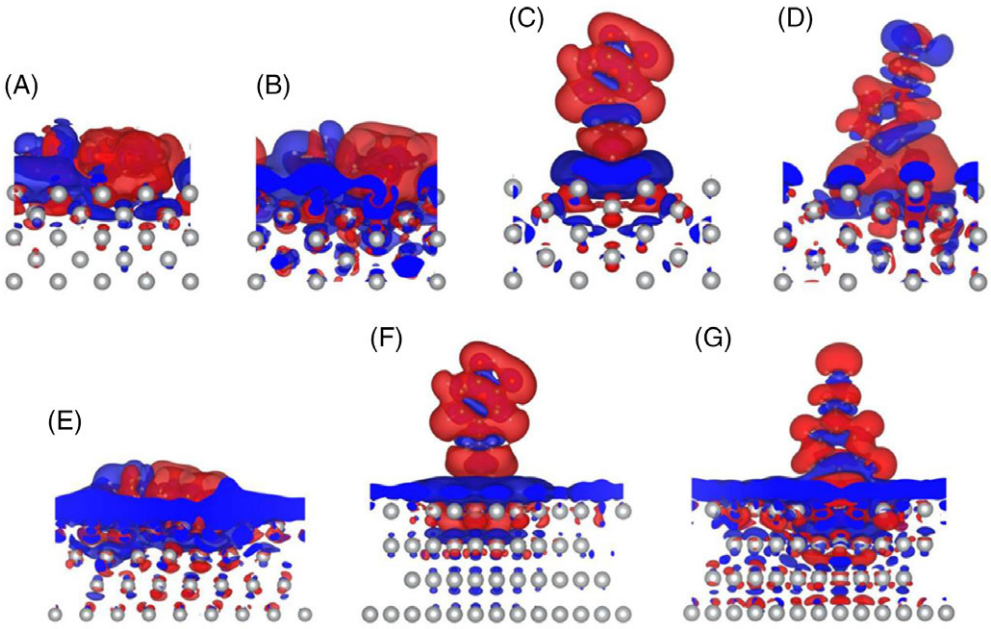

FIGURE 8 Charge density difference ($\Delta\rho$) plots for ZDA adsorbed on Ag: A, ZDA/Ag(110) S-110-a mode, B, ZDA/Ag(110) S-110-b mode, C, ZDA/Ag(110) S-110-ea mode, D, ZDA/Ag(110) P-110-oh mode, E, ZDA/Ag(111) S-111 mode, F, ZDA/Ag(111) P-111-ea mode, G, ZDA/Ag(111) P-111-oh mode. Isosurfaces corresponding to $\Delta\rho = \pm 8.10^{-5}$ bhor^{-3} are depicted. Blue regions show electron charge accumulation, and red regions, electron charge loss. Ball colors for atoms as in Figure 7

the actual $E_{elec/loc}$ value, it provides an estimation of its role in the adsorption process. Following this procedure, we obtained $E_{elec/loc}$ = −0.78 eV and $E_{elec/loc}$ = −0.54 eV, for the P-110-ea and P-111-ea sites, respectively; and $E_{elec/loc}$ = −0.63 eV and $E_{elec/loc}$ = −0.85 eV, for the P-110-oh and P-111-oh sites, respectively. E_{elec} magnitude can be compared to the sum of deformation energies, $E_{def} = E_{def/adsorbate} + E_{def/substrate}$: E_{def} = 0.90 eV and E_{def} = 0.68 eV, for the P-110-ea and P-111-ea sites, respectively; and E_{def} = 1.16 eV and E_{def} = 0.95 eV, for the P-110-oh and P-111-oh sites, respectively. We notice that this local electrostatic energy counteracts a significant fraction of the total deformation energy, contributing to the stabilization of perpendicular ZDA adsorption modes on Ag. The relevance of electrostatic interactions to account for the stabilization of adsorbed molecules on metallic surfaces was earlier considered for adenine on Cu(110).[51]

The electronic structure inherent to the ZDA/Ag system was analyzed calculating the PDOS on specific fragments of the unit cell. Figure 9 shows the PDOS on ZDA and the first layer of Ag(110). Two scenarios are compared, ZDA placed far apart from Ag(110) surface and ZDA adsorbed on Ag(110) in the S-110-a mode. Peaks corresponding to occupied molecular orbitals of ZDA move to greater binding energies. Indeed, ZDA selected levels designed as (i), (ii), and (iii) in Figure 9 show shifts of −1.08 eV, −1.18 eV, and − 0.60 eV to lower energies, respectively. These results can be associated to the presence of a positive charged region on the ZDA molecule that stabilizes the ZDA energy levels. A similar result was commented above for NDA/Ag and correlates with an electron charge transfer from adsorbate to the substrate. It can be observed that the Ag d-band is wider by about 0.25 eV on ZDA adsorption, with the presence of a broader feature in the middle of the band, at about −4.0 eV. This remark is compatible with the establishment of a coupling between the Ag d-orbitals and ZDA atomic orbitals. As it is shown in the upper panel of Figure 9, the set of levels for distant ZDA in the −5.76 to −3.54 eV range overlaps the bottom part of Ag d-band; therefore, in this situation a coupling between them and Ag d-band is to be expected. In fact, the electronic states of adsorbed ZDA in the −6.82 to −4.15 eV range, which are 0.84 eV lower in energy, can be considered as the bonding counterparts of this orbital mixing. They show a larger broadening of 2.67 eV compared to 2.22 eV for distant ZDA. If we analyze the ZDA bonding to Ag from a frontier-orbital-way perspective and note that the occupied orbitals of distant ZDA before adsorption are below the Ag Fermi level (see upper panel in Figure 9), we could say that this orbital mixing would yield a two-orbital four-electron like interaction. The coupling antibonding component may rise above the Fermi level and give its electrons to the metal surface, remaining the bonding combination filled. Therefore, the formation of an attractive interaction of covalent nature is expected to be established between adsorbate and substrate.[56]

Figure 10 shows the 2D NCI-plots for ZDA/Ag in the S-110-a and S-111 adsorption modes calculated with the charge density coming from the DFT-D2 method. We note the appearance of a somewhat steeped peak for negative and near zero values of sign(λ_2)ρ and of a more bulky peak around −0.025 a.u.

They are evidence for the presence of attractive interactions of noncovalent nature similar to those present in NDA/Ag. Furthermore, a steeped peak around −0.050 a.u. for the S-111 adsorption mode is compatible with the formation of an even stronger attractive interaction of this nature.[43] Looking at the 3D plots for negative values of λ_2 displayed in Figure 10 for both S-110-a and S-111 sites, we note the presence of green color regions associated with van der Waals interactions and light blue and blue colors regions which can be associated to the stronger noncovalent interactions. In particular, the blue color region is localized between the O^--substituent and an Ag atom of the surface.

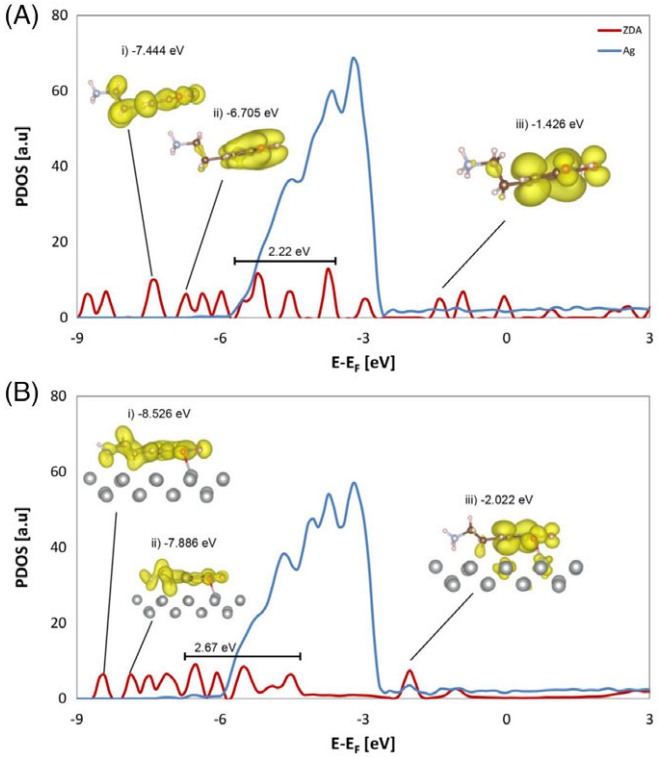

FIGURE 9 Electronic projected-DOS on the ZDA molecule (ZDA) and on the first Ag layer (Ag) of ZDA/Ag(110) system: A, ZDA molecule placed far from Ag(110), B, ZDA molecule adsorbed on Ag(110) in S-110-a mode. The insets (i) to (iii) from the left to the right display the electronic charge density (ρ) isosurfaces (5.10^{-5} bhor^{-3}) for selected levels of ZDA, respectively. The corresponding energy eigenvalues are also indicated. The horizontal bars denote the energy intervals −5.76 to −3.54 eV and − 6.82 to −4.15 eV of ZDA for cases (a) and (b), respectively. The calculations of ρ were performed at the Γpoint

3.3.3 | General discussion on the ZDA/Ag system

Taking into account the results above commented, we observe that the ZDA adsorption stacking modes behave similarly as the DA stacking modes in relation to the role played by the Ag surface coordination number. However, for ZDA adsorbed on the (110) plane, this molecule prefers to be oriented along the [100] direction. The adsorption energy magnitude is significantly larger (by about 1.5 eV) than that for the DA molecule,

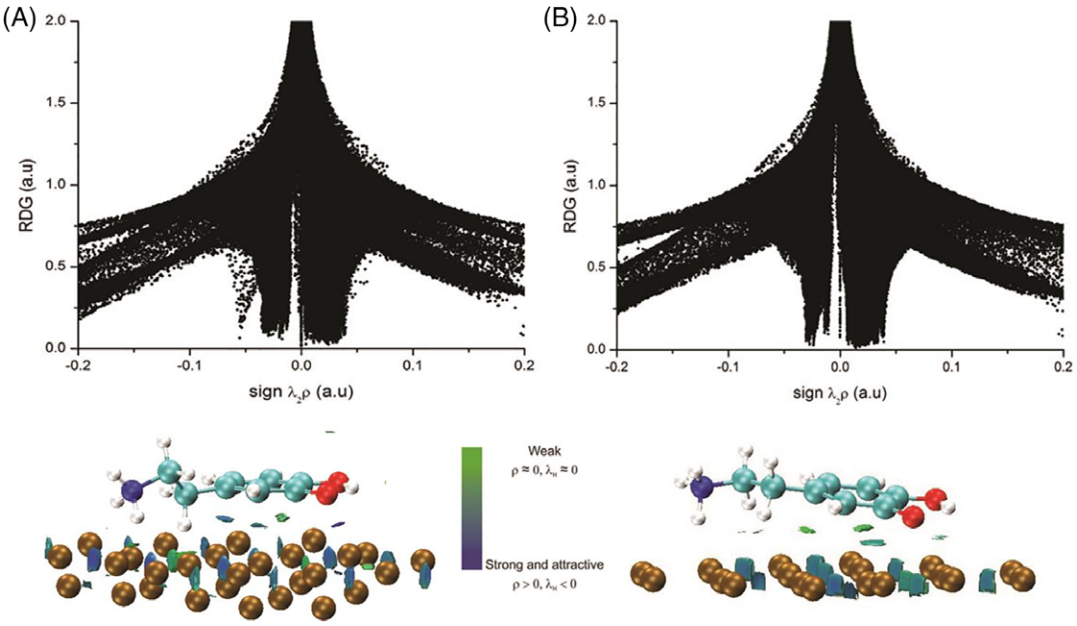

FIGURE 10 2D (left panel) and 3D (right panel, perspective view) NCI plots for ZDA adsorbed on Ag: A, ZDA/Ag(110) S-110-a mode, B, ZDA/Ag (111) S-111 mode. 3D NCI isosurfaces correspond to s = 0.25 and a color scale of $-0.1 \leq \text{sign}(\lambda_2)\rho \leq 0$ bhor^{-3}

presuming a more complex bonding mechanism. In comparison with DA/Ag where only the S-110-b mode was concerned, the internal C4-C3-C2-C1 dihedral angle for the three stacking adsorption modes for ZDA/Ag suffers a significant distortion; hence, the ethylamine group becomes reoriented toward the Ag surface and the molecule is largely deformed. The interatomic distances between the adsorbate and substrate are compatible with some degree of covalent bonding, besides other possible bonding sources. As it was performed for NDA/Ag, the analysis accomplished on different energy contributions and on electronic structure properties allowed us to quantify and identify these contributions. E_{VDW} contribution is negative, contrary to the results for NDA/Ag, indicating that this contribution adds to E_{VDW} to define the ZDA stability on the three surfaces considered. An electron transfer is produced from ZDA to Ag, whose magnitude is larger than that observed for DA/Ag, stating that a stronger ionic interaction is present between adsorbate and substrate. Moreover the projected-LDOS curves reveal that ZDA levels couple with the Ag-d band, giving rise to the system stabilization. Therefore, three sources of bonding have been identified for ZDA/Ag: ionic, covalent and noncovalent. The last are of dispersive and even much stronger nature and localized between the atoms of the aromatic ring and its substituents, specially the amino group, and the Ag substrate atoms.

All of the perpendicular adsorption modes are less favored than the stacking modes (by about 2.1 eV), indicating that the stacking modes would be the preferential modes on Ag nanoparticles. Nevertheless, they cannot be completely discarded in large coverage situations. In particular, the P-ea modes are more favored than the P-oh ones, in agreement with the formation of cross-linked noble metal nanoparticles. The aggregation of these nanoparticles would be induced by hydrogen bonding between the hydroxyls of dopamine molecules, with a simultaneous anchoring of dopamine molecule to the metal surface via amino groups. Theoretically, the perpendicular orientations exhibit significant deformation energies when compared with stacking modes. They particularly come from the substrate deformation and are counterbalanced by significant attractive energies between the NH_3^+ and O^--substituents of dipolar ZDA molecule and polarized surface Ag atoms.

It is noteworthy that ZDA as structural dopamine isomer is less stable than NDA in vacuum, but on adsorption on Ag, its bonding is stronger than that of NDA. Parallel to this, the ZDA trans-conformer here designed directly as ZDA is also less stable than the gauche-conformer G-ZDA, but on adsorption on Ag, its bonding is stronger than that of G-ZDA. In other words, in both cases, the most unfavored species in vacuum becomes the more reactive with the Ag surface.

3.4 | The vibrational spectra of neutral and zwitterionic dopamine species

In this section, the calculated vibrational frequencies corresponding to NDA and ZDA molecules adsorbed on Ag surfaces are analyzed taking into account the relevance of these values to interpret IR and Raman spectra and the interest to reveal the Ag substrate effect on free NDA and ZDA vibrational frequencies.

In Table 4, the main vibrational frequency values corresponding to free and adsorbed NDA (S-110-a, S-110-b, and S-111 sites) are summarized in decreasing order. All these results and other vibrational frequencies not reported here were obtained with the VASP code, considering the adequate unit cell for each system. With the purpose of focusing on the most relevant frequencies from the experimental point of view, the normal modes were selected taking into account the most relative intense transitions for the free molecule and the feasibility of their classification according to the standard bands for organic compounds.[59] This discrimination based on the intensity of vibrational frequencies was performed considering the results provided by the Gaussian 03 code.[25] The results of VASP vibrational frequencies obtained for free neutral dopamine have been compiled in the second column of Table 4. These frequencies can be compared to the available experimental values from Refs. [57] and [58] in the sixth to eighth columns of the same table. We note that while the FT Raman results for O-H and H-N-H stretching bands are about 300-400 cm^{-1} lower than the theoretical ones, the other measured bands are only up to 50 cm^{-1} lower. This observation could be explained by the formation of hydrogen bonds between NDA molecules. The Ag substrate produces several modifications on NDA vibrational frequencies. From Table 4, we notice that the O-H-para and O-H-metha stretching bands show large red shifts of 79-131 cm^{-1} and 121-400 cm^{-1}, respectively, with respect to the free molecule; the largest one being that of S-110-b site, revealing that the O-H bonds become weakened with respect to the free NDA molecule. These changes and those suffered by other bands are summarized systematically in Table S3 of Supporting Information. For that purpose, mean vibrational frequency values of bands with the same normal mode assignment have been calculated and reported as shifts with respect to the free molecule. Looking at Table S3, we notice that a new (< 1150 cm^{-1}) CO stretching band redshifted by 126-147 cm^{-1} appears specifically for S-110-b and S-111 sites. The lowest (< 3000 cm^{-1}) bands of methylene C-H stretching and the symmetrical (> 1520 cm^{-1}) bands of aromatic C-C stretching show smaller red shifts of up to 52 cm^{-1} and 75 cm^{-1}, respectively, for all NDA adsorption sites. Conversely, the ethyl C-C stretching normal mode of C2-C3 bond shows blue shifts of up to 61 cm^{-1}, for all adsorption sites.

In Table 5, the vibrational frequency values corresponding to free and several adsorbed ZDA geometries (S-110-a, P-110-ea, P-110-oh, S-111, P-111-ea, and P-111-oh sites) are summarized in decreasing order. Comparing the results of vibrational frequencies obtained for free zwitterionic with those of neutral dopamine, we notice significant modifications. The following ZDA frequencies ordering: N-H stretching > O-H stretching and methylene C-H stretching > aromatic C-H stretching is the inverse of that obtained for NDA. The O-H and N-H stretching frequencies undergo red shifts of 700 and 70-80 cm^{-1} with respect to NDA, respectively. Conversely, one band of C-O-H bending and one of C-O stretching undergo blue shifts of about 100 and 180 cm^{-1}, respectively. Moreover, the number of aromatic C-C stretching bands changes from four to two, and two new H-C-H out-of-plane bending bands appear.

TABLE 4 Vibrational frequencies (in cm^{-1}) for free NDA and NDA adsorbed on Ag substrate and their corresponding mode assignments

Assignment[a]	NDA	NDA/Ag(110) S-110-a	NDA/Ag(110) S-110-b	NDA/Ag (111) S-111	FTIR[b]	FT Raman[b]	FT Raman[c]
Para-O-H stretching	3677	3598	3546	3577			3345
Metha-O-H stretching	3734	3613	3334	3452			3343
Amine N-H stretching	3481 as 3395 sy	3487 as 3454 sy	3448 as 3373 sy	3484 as 3463 sy			3081 a 3054s
Methylene C-H stretching	3057 bo	3033 sy[d]	3035 sy[d]	3039 sy[d]	3004 as		
	3025 bo	3003 as[d]	3006 as[d]	3000 as[d]			
	2993 sy[d] 2970 sy[e]	2944[f] 2914[f]	2979[f] 2895[f]	2973 sy[e] 2930 as[e]	2952 sy	2968 sy	
Aromatic C-C stretching	1644 as	1581 as	1579 as	1586 as	1600 as		
	1632 as	1576 as	1567as	1581 as	1586 as		
	1517 sy	1497 sy	1483 sy	1492 sy	1501 sy		
	1445 sy	1411 sy					
C-O-H bending	1323	1379	1377	1375	1321 as	1327 as	
	1316	1322	1310	1319	1261 sy		
	1175 (O2)	1186 (O2)	1176 (O2)	1182 (O2)			
	1144 (O1)	1147 (O1)	1163 (O1)	1166 (O1)			
C-O stretching	1269	1277	1232	1252	1214 as		
	1244	1247	1135	1236	1191 sy		
	1233	1230	1110	1102			
Ethyl C-C stretching (C2-C3)	1233	1277	1281	1280			
	1113	1174	1163	1166			

[a] Key: as, asymmetrical vibration; sy, symmetrical vibration; bo, both methylene groups of ethyl chain involved in vibration.
[b] Ref. [57]
[c] Ref. [58]
[d] C1 & 2H.
[e] C2 & 2H.
[f] C2 & 1H. The experimental values correspond to pure (nonadsorbed) dopamine.

The Ag substrate causes significant modifications on ZDA vibrational frequencies, which are much more extensive than those for NDA/Ag. The changes suffered by different bands are summarized in Table S4 of Supporting Information, as it was performed in Supporting Information Table S3. Looking at Supporting Information Table S4, it is noteworthy that the highest (> 3000 cm^{-1}) amine N-H stretching bands show large red shifts of 215-263 cm^{-1} for the perpendicular configuration of adsorption, and red shifts of 144 cm^{-1} and 65 cm^{-1} for the stacking S-110-a and S-111 configurations, respectively. These results reveal that the N-H bonds become weakened on adsorption with respect to the free molecule situation. They are in agreement with the general N-H stretching above-described in section 3.3.1. Moreover, another amine N-H stretching band (for <3000 cm^{-1}) significantly redshifted by 617 and 669 cm^{-1} appears for S-110-a and S-111 sites, respectively, and by 384 cm^{-1} for the P-110-ea site. This observation is compatible with the fact that for these sites one or two N-H bonds show a larger stretching of 0.02-0.04 Å, compared with the 0.01 Å stretching for the perpendicular P-110-oh, P-111-oh, and P-111-oh sites. Note also that for the stacking configurations one mode is lower (by at least 100 cm^{-1}) and at the same time another is higher (by at least 230 cm^{-1}) than the values for the perpendicular states. This great influence on the stacking sites could be related to the much larger E_{ads} magnitude for these sites. The H-N-H in-plane bands show red shifts of up to 76 cm^{-1} for all ZDA adsorption sites. The aromatic C-C stretching band redshifted by up to 55 cm^{-1} only for the perpendicular-oh configurations.

The intermediate bands (in the 1200-1300 cm^{-1} range) of C-O-H bending in-plane normal modes redshifted by up to 74 cm^{-1} for the perpendicular-oh configurations; moreover, another C-O-H bending in-plane redshifted by 115-117 cm^{-1} appears only for perpendicular-oh configurations. Conversely, the O-H stretching band undergoes significant blue shifts of 372-428 cm^{-1} for the two perpendicular-oh and S-111 configurations and of 195-237 cm^{-1} for the other sites, revealing that for these configurations the O-H bond is strengthened with respect to the free molecule situation. This observation is in agreement with the general O-H shortening above described in section 3.1.1. The aromatic C-C-H bending and the aromatic C-H stretching bands exhibit likewise blue shifts but of lower magnitude, up to 63 cm^{-1}, for the P-110-oh and S-111 sites. The other normal modes exhibit red or blue shifts depending on the site specificity. The intermediate methylene C-H stretching bands undergo only blue shifts, of up to 103 cm^{-1} in the case of P-110-oh and the three sites of Ag(111) surface, while another methylene C-H stretching band redshifted by 83-112 cm^{-1} appears exclusively for the stacking configurations. The lowest (< 1300 cm^{-1}) H-C-H out-of-plane bands redshifted by up to 59 cm^{-1} for the P-111-ea and S-110-oh sites. Conversely, the lowest (< 1300 cm^{-1}) C-O stretching normal

TABLE 5 Vibrational frequencies (in cm^{-1}) for free ZDA and ZDA adsorbed on Ag substrate and their corresponding mode assignments

Assignment[a]	ZDA	ZDA /Ag (110) S-a	ZDA/Ag (110) P-ea	ZDA/Ag (110) P-oh	ZDA/Ag (111) S	ZDA/Ag (111) P-ea	ZDA/Ag (111) P-oh
Amine N-H stretching	3411 sy	3388	3235	3168 sy	3380 as	3187	3143 as
	3400 sy	3080	3036 sy	3104 as	3245 sy	3161	3128
	3322 as	2761	2994	3072 as	2709 sy	3115	3126 sy
O-H stretching	3008	3245	3198	3380	3436	3203	3428
Methylene C-H stretching	3091 as[b] 3022 sy[b] 2985 as[c] 2925 sy[c]	3063[d] 3036[d] 2963[e] 2843[e]	3071 as[b] 3008 sy[b] 2997 as[c] 2951 sy[c]	3082 as[b] 3062 sy[c] 3004[e] 2967[e]	3119 as[b] 3099 sy[b] 3058[e] 2872[e]	3074 as[b] 3025 sy[b] 3002 as[c] 2965 sy[c]	3087 as[b] 3066[d] 3002[c,d] 2984 as[c]
Aromatic C-H stretching	3101 3079 3074	3127 3112 3064	3125 3105 as 3084 sy	3111 sy 3095 as 3083	3181 3151 3111	3125 3103 3083	3102 3095 3087
H-N-H bending in-plane	1616 1606	1569 1545	1543 1527	1541 1529	1579 1538	1553 1552	1554 1550 1544
Aromatic C-C stretching	1588 1556	1580 1526	1573 1560	1544 1492	1582 1541	1567 1560	1587 1447
H-C-H bending in-plane	1444[b] 1421[c]	1452[b] 1417[c]	1448 bo 1424 bo	1424 bo 1443 bo	1439[b] 1393[c]	1452[b] 1425[c]	1444 bo 1422 bo
H-C-H bending out-of-plane	1317[b]	1357 bo	1334 bo	1322[b] 1258[c]	1340[b]	1336 bo 1280 bo	1330[b]
C-O-H bending in-plane	1437 1275	1425 1280	1419 1393 1235	1201	1398 1369 1158	1402 1241	1447 1230 1160
H-N-H bending out-of-plane	1412	1444	1419	1354	1423	1436	1372
C-O stretching	1428 1245	1401 1242 1235	1290	1432 1281	1257 (O1) 1244 (O2) 1200 (O2)	1488 (O1) 1472 (O2) 1298 (O2)	1293
Aromatic C-C-H bending	1095	1125	1110	1128	1102	1106	1116

[a] Key: as, asymmetrical vibration; sy, symmetrical vibration; bo, both methylene groups of ethyl chain involved in vibration.
[b] C1 & 2H.
[c] C2 & 2H.
[d] C1 & 1H.
[e] C2 & 1H.

modes show blue shifts of up to 53 cm^{-1} for the three perpendicular configurations. Finally, the ethyl C-C stretching band suffers a 58 cm^{-1} red shift for the S-111 site.

Recently, SERS spectra for zwitterionic dopamine adsorbed onto Au NPs coated with Ag have been reported for different pH conditions.[14] From these spectra, several relevant bands can be observed at 1126-1128, 1329, and 1462 cm^{-1} Among others, covering the pH = 4-11 range. When these experimental features are compared with our results for NDA and ZDA (see Tables 4 and 5), only those for ZDA become pertinent. The band at 1126-1128 cm^{-1} can be compared with our results of 1125 cm^{-1} (aromatic C-C-H bending for S-110-a site) and 1128 cm^{-1} (aromatic C-C-H bending for P-110-oh site), the band at 1329 cm^{-1} with the calculated bands at 1322 cm^{-1} (H-C-H bending out-of-plane for P-110-oh site), 1334 cm^{-1} (H-C-H bending out-of-plane for P-110-ea site), and 1336 cm^{-1} (H-C-H bending out-of-plane for P-111-ea site), and the band at 1462 cm^{-1} with the calculated bands at 1452 cm^{-1} (H-C-H bending in-plane for S-110-a site) and 1452 cm^{-1} (H-C-H bending in-plane for P-111-ea site). The comparison indicates that both stacking and perpendicular configurations could be important to define the structure of dopamine/Ag systems, although the latter are less favored from a theoretical point of view. Furthermore, a molecular ZDA-Ag_2 model was employed to study the interaction between adsorbate and substrate in Ref. [14]. It is interesting to look at the agreement between the Ref. [14] model and our Ag(110) and Ag(111) slab models. As the Ag_2 dimer binds to the negative O^- substituent of ZDA in the molecular model, only the P-110-oh and P-111-oh configurations have been considered for this comparison. The values obtained with these two models are summarized in Table 6, giving a mean discrepancy of 6 cm^{-1} if we take the magnitude of frequency differences for 12 different bands, showing very reasonable agreement between the two approaches.

From the above results, we notice that the ZDA vibrational frequencies suffer much more significant modifications on adsorption on Ag than those of NDA. The largest red or blues shifts of ZDA vibrational frequencies can be associated with longer or shorter bonds because the ZDA-Ag interplay is much stronger than the NDA-Ag one. Comparing our calculated frequencies of relatively neutral bonds for NDA and ZDA molecules with the SERS experimental data for dopamine/Ag, we infer that both stacking and perpendicular configurations for ZDA/Ag could be important to define the structure of dopamine/Ag systems.

TABLE 6 Comparison of calculated vibrational frequencies (in cm^{-1}) for ZDA adsorbed on Ag(110) and Ag(111) surfaces for perpendicular-oh sites with theoretical frequencies of Ref. [14] for the ZDA-Ag_2 system

	Vibrational frequency values for adsorbed ZDA											
Present work Exposed Ag plane	1128 (110)	1145 (110)	1160 (111)	1230 (111)	1281 (110)	1293 (111)	1322 (110)	1330 (111)	1372 (111)	1492 (110)	1541 (110)	1587 (111)
Ref. [14]	1128	1148	1169	1228	1273	1280	1323	1336	1380	1497	1539	1593

4 | CONCLUSIONS

The bonding, geometry, and vibrational spectra of neutral (NDA) and zwitterionic (ZDA) dopamine species adsorbed on Ag(110) and Ag(111) surfaces have been studied by using the DFT-D2 method, arriving at the following main conclusions:

- Concerning the stacking adsorption modes, both dopamine species prefer to adsorb on the most compact Ag(111) surface. The stability order for NDA adsorption on the Ag(110) surface is S-110-b > S-110-a; this order is inverted for ZDA.
- Whereas the adsorption energy magnitude of NDA on Ag for the stacking modes corresponds to a relative important adsorbate-substrate bonding, that of ZDA on Ag is significantly larger than that obtained for NDA species.
- Both molecules are electron donors to the Ag surface, giving rise to an ionic attractive interaction between adsorbate and substrate; this effect is more relevant in the case of ZDA/Ag.
- The main source of bonding for NDA/Ag comes from noncovalent interactions, while for ZDA/Ag a non-negligible coupling between ZDA and Ag atomic orbitals can also be observed.
- Perpendicular geometries for ZDA/Ag are less favored than the stacking modes; the perpendicular-ea sites being 0-3-0.6 eV relatively more favored than the perpendicular-oh ones.
- ZDA vibrational frequencies undergo noticeable red/blue shifts on adsorption on Ag which can be rationalized considering the corresponding bond strengths.

The theoretical results obtained in the present work help to attain better comprehension and analysis of experiments where dopamine species are adsorbed on noble metal surfaces, such as those of Ag nanoparticles in SERS experiments, particularly regarding Raman spectra interpretation. We also notice that all results would be helpful in other contexts where dopamine-noble metal interaction is present, such as the case of dopamine detection with gold electrods.[60]

ACKNOWLEDGMENTS

The authors want to acknowledge the financial support of these Argentine institutions: Consejo Nacional de Investigaciones Científicas y Técnicas, Agencia Nacional de Promoción Científica y Tecnológica, and Universidad Nacional del Sur, the last two under Grants PICT-2014-1778 and PGI 24/F063, respectively.

ORCID

Norberto J. Castellani https://orcid.org/0000-0003-2432-116X

REFERENCES

[1] P. Seeman, in *Historical Overview: Introduction to the Dopamine Receptors* (Ed: K. A. Neve), Humana Press, Totowa, NJ **2010**, p. 1.
[2] M. L. Heien, A. S. Khan, J. L. Ariansen, J. F. Cheer, P. E. M. Phillips, K. M. Wassum, R. M. Wightman, *Proc. Natl. Acad. Sci. USA* **2005**, *102*, 10023.
[3] J. Birtwistle, D. Baldwin, *Br. J. Nurs.* **1998**, *7*, 832.
[4] J. Granot, *FEBS Lett.* **1976**, *67*, 271.
[5] D. C. Li, P. H. Yang, M. S. C. Lu, *IEEE Trans. Electron Devices* **2010**, *57*, 2761.
[6] L. Wu, L. Feng, J. Ren, X. Qu, *Biosens. Bioelectron.* **2012**, *34*, 57.
[7] Q. Mu, H. Xu, Y. Li, S. Ma, X. Zhong, *Analyst* **2014**, *139*, 93.
[8] Y. Bu, S. Lee, *ACS Appl. Mater. Interfaces* **2012**, *4*, 3923.
[9] S. R. Palanisamy, X. Zhang, T. He, *Sci. China Chem.* **2015**, *58*, 0.
[10] B. Sharma, R. R. Frontiera, A.-I. Henry, E. Ringe, R. P. Van Duyne, *Mater. Today* **2012**, *15*, 16.
[11] S. L. Kleinman, E. Ringe, N. Valley, K. L. Wustholz, E. Phillips, K. A. Scheidt, G. C. Schatz, R. P. Van Duyne, *J. Am. Chem. Soc.* **2011**, *133*, 4115.
[12] Y. Bu, S. W. Lee, *J. Nanosci. Nanotechnol.* **2013**, *13*, 5992.
[13] Y. Zhang, B. Li, X. Chen, *Microchim. Acta.* **2010**, *168*, 107.
[14] S. Pande, S. Jana, A. K. Sinha, S. Sarkar, M. Basu, M. Pradhan, A. Pal, J. Chowdhury, T. Pa, *J. Phys. Chem. C.* **2009**, *113*, 6989.
[15] R. I. Masel, *Principles of Adsorption and Reaction on Solid Surfaces; Wiley Series in Chemical Engineering*, Wiley, New York **1996**.
[16] J. Koryta, W. Dvorak, L. Kavan, *Principles of Electrochemistry*, 2nd ed., Wiley, New York **1993**.
[17] F. Schedin, A. K. Geim, S. V. Morozov, E. W. Hill, P. Blake, M. I. Katsnelson, K. S. Novoselov, *Nat. Mater.* **2007**, *7*, 652.
[18] Y. Shao, J. Wang, H. Wu, J. Liu, I. A. Aksay, Y. Lina, *Electroanalysis* **2010**, *22*, 1027.

[19] Q. Feng, W. Zhao, S. Wen, Q. Cao, *Sep. Purif. Technol.* **2017**, *178*, 193.
[20] Q. Feng, W. Zhao, S. Wen, *Appl. Surf. Sci.* **2018**, *436*, 823.
[21] B. Hammer, J. K. Nørskov, *Adv. Catal.* **2000**, *45*, 71.
[22] W. Liu, A. Tkatchenko, M. Scheffler, *Acc. Chem. Res.* **2014**, *47*, 3369.
[23] M. A. Hall, C. Mui, C. B. Musgrave, *J. Phys. Chem. B* **2001**, *105*, 12068.
[24] Q. Feng, S. Wen, J. Deng, W. Zhao, *Appl. Surf. Sci.* **2017**, *396*, 920.
[25] Q. Feng, S. Wen, J. Deng, W. Zhao, *Appl. Surf. Sci.* **2017**, *425*, 8.
[26] S. Kilina, S. Tretiak, D. A. Yarotski, J.-X. Zhu, N. Modine, A. Taylor, A. V. Balatsky, *J. Phys. Chem. C* **2007**, *111*, 14541.
[27] C. R. L. Chapman, E. C. M. Ting, A. Kereszti, I. PaciJ, *J. Phys. Chem. C* **2013**, *117*, 19426.
[28] I. Karki, H. Wang, N. R. Geise, B. W. Wilson, J. P. Lewis, T. Gullion, *J. Phys. Chem. B* **2015**, *119*, 11998.
[29] Z. Yang, Y.-P. Zhao, *Eng. Anal. Bound. Elem.* **2007**, *31*, 402.
[30] G. Kresse, J. Furthmüller, *Comput. Mater. Sci.* **1996**, *6*, 15.
[31] G. Kresse, J. Furthmüller, *Phys. Rev. B* **1996**, *54*, 11169.
[32] J. P. Perdew, K. Burke, M. Ernzerhof, *Phys. Rev. Lett.* **1996**, *77*, 3865.
[33] P. E. Blöchl, *Phys. Rev. B* **1994**, *50*, 17953.
[34] G. Kresse, D. Joubert, *Phys. Rev. B* **1999**, *59*, 1758.
[35] F. Y. Alzoubi, J. Y. Alzouby, M. K. Alqadi, H. A. Alshboul, K. M. Aljarrah, *Chin. J. Phys.* **2015**, *53*, 100801.
[36] M. Vanaja, G. Gnanajobitha, K. Paulkumar, S. Rajeshkumar, C. Malarkodi, G. Annadurai, *J. Nanostruct. Chem.* **2013**, *3*, 17.
[37] A. Henglein, M. Giersig, *J. Phys. Chem. B* **1999**, *103*, 9533.
[38] L. A. Meier, N. J. Castellani, *Comput. Mater. Sci.* **2017**, *127*, 48.
[39] S. Grimme, J. Antony, S. Ehrlich, H. Krieg, *J. Chem. Phys.* **2010**, *132*, 1.
[40] M. J. Frisch, G. W. Trucks, H. B. Schlegel, G. E. Scuseria, M. A. Robb, J. R. Cheeseman, J. A. Montgomery Jr.. , T. Vreven, K. N. Kudin, J. C. Burant, J. M. Millam, S. S. Iyengar, J. Tomasi, V. Barone, B. Mennucci, M. Cossi, G. Scalmani, N. Rega, G. A. Petersson, H. Nakatsuji, M. Hada, M. Ehara, K. Toyota, R. Fukuda, J. Hasegawa, M. Ishida, T. Nakajima, Y. Honda, O. Kitao, H. Nakai, M. Klene, X. Li, J. E. Knox, H. P. Hratchian, J. B. Cross, V. Bakken, C. Adamo, J. Jaramillo, R. Gomperts, R. E. Stratmann, O. Yazyev, A. J. Austin, R. Cammi, C. Pomelli, J. W. Ochterski, P. Y. Ayala, K. Morokuma, G. A. Voth, P. Salvador, J. J. Dannenberg, V. G. Zakrzewski, S. Dapprich, A. D. Daniels, M. C. Strain, O. Farkas, D. K. Malick, A. D. Rabuck, K. Raghavachari, J. B. Foresman, J. V. Ortiz, Q. Cui, A. G. Baboul, S. Clifford, J. Cioslowski, B. B. Stefanov, G. Liu, A. Liashenko, P. Piskorz, I. Komaromi, R. L. Martin, D. J. Fox, T. Keith, M. A. Al-Laham, C. Y. Peng, A. Nanayakkara, M. Challacombe, P. M. W. Gill, B. Johnson, W. Chen, M. W. Wong, C. Gonzalez, J. A. Pople, *Gaussian 03 (Revision D.01)*, Gaussian, Inc., Wallingford, CT **2004**.
[41] T. A. Manz, N. Gabaldon Limas, *RSC Adv.* **2016**, *6*, 47771.
[42] E. R. Johnson, S. Keinan, P. Mori Sánchez, J. Contreras García, A. J. Cohen, W. Yang, *J. Am. Chem. Soc.* **2010**, *13*, 6498.
[43] A. Otero-de-la-Roza, E. R. Johnson, J. Contreras-García, *Phys. Chem. Chem. Phys.* **2012**, *14*, 12165.
[44] K. Momma, F. Izumi, *J. Appl. Crystallogr.* **2011**, *44*, 1272.
[45] W. Humphrey, A. Dalke, K. Schulten, *J. Mol. Graph.* **1996**, *14*, 33. See http://www.ks.uiuc.edu/Research/vmd/.
[46] E. P. A. Couzijn, J. C. Slootweg, A. W. Ehlers, K. Lammertsma, *J. Am. Chem. Soc.* **2010**, *132*, 18127–18140. See http://www.jmol.org/.
[47] R. Fausto, M. J. S. Ribeiro, J. J. P. De Lima, *J. Mol. Struct.* **1999**, *484*, 181.
[48] P. I. Nagy, K. Takács-Novák, *Phys. Chem. Chem. Phys.* **2004**, *6*, 2838.
[49] R. Bergin, D. Carlström, *Acta Cryst.* **1968**, *B24*, 1506.
[50] D. P. Miller, S. Simpson, N. Tymińska, E. Zurek, *J. Chem. Phys.* **2015**, *142*, 101924.
[51] E. Rauls, S. Blankenburg, W. G. Schmidt, *Surf. Sci.* **2008**, *602*, 2170.
[52] D. Bogdan, C. Morari, *J. Phys. Chem. C* **2012**, *116*, 7351.
[53] A. C. Rossi Fernández, N. J. Castellani, *Chemphyschem* **2017**, *18*, 2065.
[54] F. Ortmann, W. G. Schmidt, F. Bechstedt, *Phys. Rev. Lett.* **2005**, *95*, 186101.
[55] M. Preuss, W. G. Schmidt, F. Bechstedt, *Phys. Rev. Lett.* **2005**, *94*, 236102.
[56] R. J. Hoffman, *Solid and Surfaces: A Chemist's View of Bonding in Extended Structures*, VCH Publishers, Inc., New York **1988**, p. 68.
[57] S. Gunasekaran, R. Thilak Kumar, S. Ponnusamy, *Indian J. Pure Appl. Phys.* **2007**, *45*, 884.
[58] S. K. Park, N. S. Lee, S. H. Lee, *Bull. Korean Chem. Soc.* **2000**, *21*, 959.
[59] B. H. Stuart, in *Organic Molecules; in Infrared Spectroscopy: Fundamentals and Applications* (Ed: D. J. Ando), Wiley, Chichester **2004**, p. 71.
[60] M. K. Zachek, A. Hermans, R. M. Wightman, G. S. McCarty, *J. Electroanal. Chem.* **2008**, *614*, 113.

SUPPORTING INFORMATION

Additional supporting information may be found online in the Supporting Information section at the end of the article.

How to cite this article: Rossi-Fernández AC, Meier LA, Castellani NJ. Neutral and zwitterionic dopamine species adsorbed on silver surfaces: A DFT investigation of interaction mechanism. *Int J Quantum Chem*. 2018;e25817. https://doi.org/10.1002/qua.25817